Article:
Moneo-Sánchez, M, Alonso-Chico, A, Knox, JP et al. (2019) β-(1,4)-Galactan remodelling in Arabidopsis cell walls affects the xyloglucan structure during elongation. Planta, 249 (2). pp. 351-362. ISSN: 0032-0935

https://doi.org/10.1007/s00425-018-3008-5

María Moneo-Sánchez[1], Alejandro Alonso-Chico[1], J. Paul Knox[2], Berta Dopico[1], Emilia Labrador*[1], Ignacio Martín[1]

β-(1,4)-Galactan Remodelling in Arabidopsis Cell Walls Affects the Xyloglucan Structure During Elongation"

[1]Instituto Hispano-Luso de Investigaciones Agrarias (CIALE). Dpto de Botánica y Fisiología Vegetal. Facultad de Biología. Universidad de Salamanca. Campus Miguel de Unamuno. 37007, Salamanca (Spain).

[2]Centre for Plant Sciences, Faculty of Biological Sciences, University of Leeds, LS2 9JT (United Kingdom).

*Corresponding Author: email: labrador@usal.es; Telephone: +34 923 294471; Fax: +34 923 294515.

Main conclusion:

Galactan turnover occurs during cell elongation and affect the cell wall xyloglucan structure which is involved in the interaction between cellulose and xyloglucan.

Abstract:

β-(1,4)-galactan is one of the main side chains of rhamnogalacturonan I. Although the specific function of this polymer has not been completely established, it has been related to different developmental processes. To study β-(1,4)-galactan function we have generated transgenic Arabidopsis plants overproducing chickpea βI-Gal β-galactosidase under the 35S CaMV promoter (35S:: βI-Gal) to reduce galactan side chains *in muro*. Likewise, an Arabidopsis double loss-of-function mutant for BGAL1 and BGAL3 Arabidopsis β-galactosidases (*bgal1/bgal3*) has been obtained in order to increase galactan levels.

The characterization of these plants has confirmed the role of β-(1,4)-galactan in cell growth, and demonstrated that the turnover of this pectic side chain occur during cell elongation, at least in Arabidopsis etiolated hypocotyls and floral stem internodes. The results indicate that BGAL1 and BGAL3 β-galactosidases act in a coordinate way during cell elongation. Additionally, this work indicates that galactan plays a role in the maintenance of the cell wall architecture during this process. Our results point to an involvement of the β-(1,4)-galactan in the xyloglucan structure and the interaction between cellulose and xyloglucan.

Keywords: β-galactosidases, growth, pectin

Acknowledgements: The work was founding by the Spanish Ministerio de Economía y Competitividad (MINECO) [BFU2013-44793-P] and for the Junta de Castilla-León (SA027G18). M. Moneo-Sánchez was supported by Programa Predoctoral de Formación de Personal Investigador grant from the Basque Government. Generation of the CCRC series of monoclonal antibodies used in this work was supported by a grant from the National Science Foundation **(**NSF) Plant Genome Program [DBI-0421683].

Introduction

Cell walls are one of the key factors controlling growth and morphogenesis in plants. The primary cell wall of dicotyledonous plants is composed of a complex mixture of different polymers, with a notable role of polysaccharides, particularly cellulose, xyloglucan (XG) and pectins.

Several structural models have been proposed to explain how the different cell wall polysaccharides interact with each other (McCann and Roberts 1991; Talbott and Ray 1992; Carpita and Gibeaut 1993). All of them assume the existence of two structurally independent but interrelated domains: the cellulose-XG network and the pectic polysaccharides. According to some classical models (Hayashi 1989; Carpita and Gibeaut 1993) pectins seemed to act as a gel-like matrix in which the cellulose-xyloglucan network is embedded. In these models, the cellulose-XG domain is the important factor for the maintenance of the cell wall structure, whereas the pectic polysaccharides would be controlling the porosity of the apoplastic space, thus limiting the access of the enzymes and other macromolecules to their sites of action and regulating the assembly and reorganization of the different components of the cell wall (O'Neill and York 2003).

However, more recent studies indicate that only a small amount of XG is bound to cellulose microfibrils (Dick-Pérez et al. 2011; Cosgrove 2016). It has also been suggested that the lower interaction between these polymers could be due to a greater interaction of XG with pectins, which would be either directly linking with XG or blocking the access of XG to cellulose (Park and Cosgrove 2015). Thus, pectins could be coating XG and establishing covalent bonds probably through rhamnogalacturonan I (RGI) side chains, mainly arabinans and galactans (Popper and Fry 2008). Similarly, Wang et al. (2015) have confirmed the previously proposed pectin-cellulose interactions, which may be also occurring through the neutral side chains of RGI (Zykwinska et al. 2007; Lin et al. 2015). All these connections between pectins and other cell wall components must be considered to explain cell wall dynamics during growth and reinforce the importance of the arabinan and galactan pectic side chains in the structural maintenance of the cell wall.

The importance of the cellulose-XG network controlling cell wall loosening during growth has been extensively documented (Pauly et al. 2001; Cosgrove 2016) and different proteins such as α-expansins or XTH (xyloglucan endotransglycosylase/hydrolase) (Miedes et al. 2011; Wang et al. 2013) have been reported to be responsible for rearrangement of the cellulose-XG domain. Also, the

pectin remodelling is increasingly apparent as a determining event during cell growth (Peaucelle et al. 2012; Wolf and Greiner 2012). In addition to the well-established role of homogalacturonan methyl-esterification and calcium cross linking in cell wall relaxation and stiffening (Willats et al. 2001), RGI side chains and more specifically β-(1,4)-galactan, are subjected to modifications during cell elongation processes (McCartney et al. 2003; Martín et al. 2013)

Different β-galactosidases have been related to β-(1,4)-galactan turnover during cell wall remodelling. Plant β-galactosidases (EC 3.2.1.23) are coded in several plant species as multigene families and each member may have specific functions in different developmental processes. Thus, some of the 17 β-galactosidases described in *Arabidopsis thaliana*, in particular the 5 β-galactosidases belonging to subfamily a1 (BGAL1, BGAL2, BGAL3, BGAL4 and BGAL5) which have been located in the cell wall (Moneo-Sánchez et al. 2016), have been related to different developmental processes during cell expansion, vegetative organ elongation or cell wall stiffening (Ahn et al. 2007; Albornos et al. 2012; Moneo-Sánchez et al. 2016). Similarly, in *Cicer arietinum*, four cell wall β-galactosidases, βI-Gal, βIII-Gal, βIV-Gal and βV-Gal (Esteban et al. 2005), have been proposed to act in pectin remodelling in processes such as cell division and elongation, primary cell wall thickening and secondary cell wall deposition or vascular cell differentiation (Martín et al. 2008, 2009, 2011, 2013).

Although pectins and specifically β-(1,4)-galactan seems to be a key factor in cell wall remodelling through development, the role of this pectic polysaccharide in cell wall architecture during cell elongation remains unknown. Here we present data of the alterations caused in Arabidopsis cell walls when β-(1,4)-galactan content is reduced or in excess. For this purpose, and using β-galactosidases as a tool, we have followed two different approaches: generation of transgenic Arabidopsis plants overproducing chickpea βI-Gal β-galactosidase under *35S* CaMV promoter (35S::βI-Gal), in order to reduce galactan side chains *in muro*, and obtaining of a double loss-of-function mutant in Arabidopsis for Arabidopsis BGAL1 and BGAL3 β-galactosidases (*bgal1/bgal3*), as a means of increasing galactan levels. All these β-galactosidases share as common feature the presence of a lectin-like domain (Ahn et al. 2007; Esteban et al. 2005), which is thought to increase the catalytic efficiency of these enzymes (Trainotti et al. 2001). The characterization of 35S:: βI-Gal and *bgal1/bgal3* plants has provided insight into the role of β-(1,4)-galactan in cell wall organization and also into the function of BGAL1 and BGAL3 in plant development.

Materials and Methods

Plant material and growth conditions

Arabidopsis thaliana Columbia (Col) ecotype was used as wild type background for T-DNA insertion mutants and genetic transformation. Seeds from WT and *bgal* mutants were surface sterilized as described by Albornos et al. (2012) and cold treated at 4 ºC for 3 d before sowing. Seeds were grown in Petri dishes on one-half-strength Murashige and Skoog (1962) agar medium with 1% (w/v) sucrose. Plates were maintained in a growth chamber (Aralab, Portugal) at 22 ºC with both a 16-h photoperiod (provided by cool-white fluorescent tubes, an irradiance of approximately 80-100 µmol m^{-2} s^{-1}), or in darkness to obtain etiolated seedlings. To obtain adult plants, 10-d-old green seedlings were transferred to plastic pots containing a 3:1 mixture of potting soil and Vermiculite and grown under the same conditions.

Molecular analysis of *bgal1/bgal3* double mutant

bgal1 (SALK_032664) and *bgal3* (SALK_019604) mutants were generated by the Salk Institute Genomic Analysis Laboratory (http://signal.salk.edu) (Alonso et al. 2003) and obtained through the Nottingham Arabidopsis Stock Centre. Homozygous lines for the T-DNA insertion were selected by using gene-specific primers in combination with the T-DNA left border-specific primer as indicated in Moneo-Sánchez et al. (2018). The single mutants were crossed to generate the double *bgal1/bgal3* mutant. The F1 was allowed to self-fertilize and the double mutant F2 plants were genotyped by PCR with the same primers used in single mutant characterization (listed in Supplementary Table S1). Once a homozygous double mutant line was selected, the absence of transcripts for each mutated gene were analysed by reverse-transcription PCR, as indicated in Moneo-Sánchez et al. (2018).

Construction of expression vectors and plant transformation

35S::CarBGal1 construct were prepared using Gateway® cloning technology (Invitrogen, USA), according to manufacturer's instructions. *Cicer arietinum CarBGal1* cDNA, coding for βI-Gal β-galactosidase, was amplified by PCR adding the attB1 and attB2 sequences at 5'- and 3'-ends, respectively. The amplified products were gel purified and used in BP reaction with pDONR201, and the entry clones generated were used in LR reaction with pK7WG2, to allow *CarBGal1* expression

under *35S* promoter (Karimi et al. 2007). All constructs were verified by sequencing. The primers used are listed on Supplementary Table S1.

The generated *35S::CarBGal1* construct was electroporated into *Agrobacterium tumefaciens* strain C5851m and *A. thaliana* plants were transformed by floral dip method (Clough and Bent 1998). Seeds harvested from infiltrated plants were screened on the appropriate antibiotic and resistant seedlings (T1) were selected.

Single insertion transformant T2 plants were screened by Southern blot according to the method described by Esteban et al. (2005), using the complete *CarBGal1* ORF as probe. The highest expressor line (named 35S::βI-Gal) was selected by reverse-transcription semi-quantitative PCR (RT-sqPCR) using *ACT2* as internal control (primers listed on Supplementary Table S1).

Preparation of cell wall extracts

Apical, actively elongating, floral stem internodes from 28-d-old WT, 35S:: βI-Gal and *bgal1/bgal3* plants and etiolated hypocotyls from 4-d-old WT, 35S:: βI-Gal and *bgal1/bgal3* seedlings were used for cell wall extracts preparation, according to the method described by Cornuault et al. (2014), with the following specifications: in all cases 1 mg of freeze-dried material was ground in a Retsch mixer mill MM400 (Sarstedt, Germany) at 30 oscillations per s for 2 min. Cell wall components were extracted sequentially with 500 µl H_2O during 20 min in a mixer mill at 30 oscillations per s. After centrifugation at 14.000xg for 12 min, the supernatant was collected and the remaining material was further extracted with 500 µl of 50 mM CDTA, pH 7.5 at the same conditions, and the same procedure was followed to obtain the KOH extract by using 500 µl of 4 M KOH containing 1% w/v $NaBH_4$. The pH of KOH extract was neutralized with 80% v/v acetic acid. All samples were stored at 20ºC until use. The remaining residue was considered the cellulosic fraction.

Analysis of the galactose content of cell walls

The neutral monosaccharide composition of the cell walls of apical floral stem internodes from 28-d-old WT, 35S:: βI-Gal and *bgal1/bgal3* plants and etiolated hypocotyls from 4-d-old WT, 35S:: βI-Gal and *bgal1/bgal3* seedlings, was analysed by gas chromatography, in order to know their galactose content. For this purpose, cell walls extracts were hydrolyzed with 2 N trifluoroacetic acid for 90 min at

121ºC. The hydrolyzed sugars were converted into alditol acetates according to Albersheim et al. (1967). A Konik 3000-HRGC device equipped with a column of 3% ECNSS-M on Gas Chrom P (Konik Instruments, Spain) was employed. Inositol was used as an internal standard.

Analysis of the cellulosic fraction

The cellulosic fraction obtained as indicated above was washed consecutively with 70% ethanol (repeated twice) and H_2O for 20 min and centrifuged at 14.000xg for 12 min after each wash. The cellulosic residue was then incubated with a cellulose-specific endoglucanase from *Aspergillus niger* (Megazyme, Ireland) using 18 U in 300 µl 0.1 M Na-acetate buffer pH 4.5 (containing 0.02% sodium azide) at 37ºC for 48 h. For all samples, a control with no enzyme was performed in the same conditions. The sugars released to the incubation media were collected by centrifugation at 14.000xg for 20 min, neutralised with 1 M Na_2CO_3 and analysed by ELISA as described below.

The neutral monosaccharide composition of the residue obtained after the enzymatic reaction was analysed by gas chromatography. For this purpose, the pellet was washed with H_2O and acetone and solubilized with 75% H_2SO_4 v/v for 90 min at RT and hydrolysed with 1 N H_2SO_2 for 2 h at 100ºC. After neutralizing with saturated $Ba(OH)_2$ the sugars were prepared for gas phase chromatography as indicated above.

Epitope detection chromatography

For epitope detection chromatography (EDC) of the polysaccharides present in the different cell wall extracts, the method described in Cornuault et al. (2014) was followed, with the specifications detailed below.

Anion-exchange chromatography. Aliquots (50 µl) of the CDTA or KOH extracts (diluted in 2.5 ml H_2O) were eluted through a 1 ml Hi-Trap ANX FF column (GE Healthcare, U.K.) using a BioLogic LP system (Bio-Rad, USA). Samples were eluted at 1 ml/min with 20 mM sodium acetate buffer, pH 4.5, from 0-2 min, with a step change, followed by a linear gradient from 0% to 50% 0.6 M NaCl in 50 mM sodium acetate buffer, pH 4.5 to 25 min, followed by 50% to 100% 0.6 M NaCl to 31 min, and 0.6 M NaCl to 48 min (Fig. S1). The fractions were neutralyzed by adding 50 µl of 1 M Na_2CO_3, and 100 µl aliquots were incubated in NUNC Maxisorp microtitre plate wells (Thermo Fisher Scientific, USA) overnight at 4°C prior to ELISA analysis of fractions in identically processed microtitre plates.

ELISA assays. After overnight incubation at 4°C, microtitre plates were washed six times with H_2O and shaken dry. Microtitre plate wells were blocked using 200 µl per well of 5% w/v milk powder in PBS (137 mM NaCl, 2.7 mM KCl, 10 mM Na_2HPO_4, 2 mM KH_2PO_4) for 2 h at room temperature. After washing, primary antibodies were added at at 1:25 dilution in 5% w/v milk powder/PBS, and incubated for 1 h. Plates were washed six times with H_2O, shaken dry, and incubated with 100 µl per well of secondary antibody (anti-rat or anti-mouse horseradish peroxidase-conjugated IgG; Sigma-Aldrich, USA) at 1:1000 dilution in 5% milk/PBS for 1 h at room temperature. After extensive washing in H_2O, plates were developed using 100 µl of substrate per well (0.1 M sodium acetate buffer, pH 6, 1% tetramethyl benzidine, 0.006% H_2O_2). The enzyme reaction was stopped by adding 50 µl of 2.5 M H_2SO_4 to each well, and the absorbance read at 450 nm.

Antibodies used

Three rat monoclonal antibodies were used in this study: anti-galactan LM5 (specific for four consecutive β-(1,4)-galactose residues), anti-xyloglucan LM25 (recognizing XLLG, XXLG and XXXG), anti-xylan/arabinoxylan LM11, anti-un-esterified homogalacturonan (LM19), anti-partially methyl-esterified homogalacturonan JIM7 and anti-arabinan BR12. These monoclonal antibodies and detailed information about them are available at PlantProbes (http://www.plantprobes.net). In addition, four mouse monoclonal antibodies against different XG substitutions were used: anti-fucosylated XG (XXFG) CCRC-M1; anti-galactosylated XG (XLLG) CCRC-M58; CCRC-M100, which recognizes XG with no xylose substitutions (XXXG); and CCRC-M101, specific for XG with xylose substitutions and no affinity to XXXG motifs. These antibodies were purchased at CarboSource Services (http://www.carbosource.net). The nomenclature proposed by Fry et al. (1993) for XG substitutions is used in this work.

Immunolocalization of cell wall polysaccharides

Immunofluorescence labelling of cell wall polysaccharides was conducted in cross sections of apical stem internodes and etiolated hypocotyls. Sample preparation and incubation with antibodies were performed as described in Moneo-Sánchez et al. (2018). LM5 Ab and secondary antibody (goat anti-rat IgG conjugated with fluorescein isothiocyanate, FITC) (Sigma-Aldrich, USA) were applied at 1:15 and 1:300 dilutions, respectively. When necessary, sections were counterstained with Calcofluor

White (0.2 µg/mL) (Fluorescent Brightner 28, Sigma, USA) for 5 min and washed 3 times before mounting in Citifluor (Citifluor AF1, Agar Scientific, UK). Images were taken using a Leica DM 4000 LED equipped with Leica DFC550 camera (Leica Microsystems, Germany).

Results

An increase of β-(1-4)-galactan caused reduced elongation in *bgal1/bgal3* floral stem internodes and etiolated hypocotyls

The role of cell wall β-(1,4)-galactan in cell elongation was studied in Arabidopsis plants by altering the levels of this polymer *in muro*. As an attempt to reduce galactan side chains, transgenic Arabidopsis plants overexpressing chickpea *CarBGal1* (coding for βI-Gal β-galactosidase) under 35S CaMV promoter have been generated. Several lines with a single insertion and with high transcripts levels of the transgene were obtained (data not shown). Two lines were selected for morphological and cell wall analyses (Fig. S2). Since results were similar in both cases, only results for one of these lines (line 3.5.4, referred hereon as 35S::βI-Gal) are shown in this work. These transgenic 35S:: βI-Gal plants showed no significant morphological differences when compared to WT (Fig. S3).

In order to increase the cell wall β-(1,4)-galactan content we have obtained a double Arabidopsis loss-of-function mutant for BGAL1 and BGAL3 β-galactosidases (*bgal1/bgal3*) by crossing single *bgal1* and *bgal3* T-DNA mutants. Once a homozygous line was selected and the absence of *AtBGAL1* and *AtBGAL3* transcripts was verified by PCR (Fig. S4), morphological characterization of *bgal1/bgal3* double mutant at different stages of development indicated that the absence of BGAL1 and BGAL3 causes a reduction in the length of the actively growing organs, such as internodes of the floral stem (Fig. 1a, Fig.S3) and etiolated hypocotyls (more pronounced in 4-d-old hypocotyls) (Fig. 1b).

Cell wall extracts from 35S::βI-Gal and *bgal1/bgal3* plants show altered galactan levels

To assess that both transgenic 35S::βI-Gal plants and *bgal1/bgal3* double mutant present alteration in their β-(1-4)-galactan levels, and establish the putative relation of this polysaccharide with elongation, an analysis of the galactose content of the cell wall and a deeper cell wall pectin characterization of most actively elongating organs, i.e. apical floral stem internodes and 4-d-old etiolated hypocotyls from both sets of plants were conducted.

As seen in table 1, the galactose content in WT apical floral internodes account for 17% of total non cellulosic cell wall monosaccharides, while in 35S::βI-Gal plants this content is reduced to 10% and is significantly increased in *bgal1/bgal3* internodes, up to a 31% of total monosaccharides. In 4-d-old hypocotyls, only significant variations were observed in the *bgal1/bgal3* double mutant, with a 30% increase in galactose content with respect to the WT.

For pectin characterization, cell wall extracts of WT, 35S::βI-Gal and *bgal1/bgal3* plants were obtained by sequential extraction with H_2O, CDTA and KOH, and the pectin-enriched CDTA fractions were analysed by epitope detection chromatography (EDC). This method, which combines the chromatographic separation of the polysaccharides present in the extract and the use of epitope-specific monoclonal antibodies in ELISA assays (Cornuault et al. 2014), allow us the identification of different subpopulations for each polymer.

The CDTA fractions were assayed with LM5 anti-galactan monoclonal antibody (Fig. 2). In apical floral stem internodes, with active elongation, two different β-(1,4)-galactan subpopulations were detected in CDTA extracts of cell walls from WT, 35S::□βI-Gal and *bgal1/bgal3*: an earlier eluting subpopulation and a more acidic one. In 35S::βI-Gal plants, a strong β-(1,4)-galactan reduction was detected in both galactan subpopulations with respect to the WT (Fig. 2a), while *bgal1/bgal3* double mutant shows increased galactan levels only in the more acidic subpopulation with a wider peak than in WT (Fig. 2a). To ensure that the differences between WT and *bgal/bgal3* mutant are statistically significant, the area under the most acid subpopulations (fraction 35-48) were calculated. Difference between the average areas for WT and *bgal/bgal3*, respectively, which represent a 21% increase, was assessed as significant with a p-value below 0.001.

Cell wall CDTA fraction from WT elongating 4-d-old etiolated hypocotyls show very low levels of β-(1,4)-galactan (Fig. 2b) with respect to floral stem internodes. No changes in β-(1,4)-galactan in 35S::βI-Gal hypocotyls regarding to WT were observed, probably due to the low levels of this polymer in WT. In *bgal1/bgal3* hypocotyls, these levels increase significantly, as indicate by LM5 signal in CDTA extracts from this organ (Fig. 2b).

When CDTA fractions were analysed using a set of monoclonal antibodies against different pectic epitopes, such as un-esterified homogalacturonan (LM19), partially methyl-esterified homogalacturonan (JIM7) or arabinan (BR12), no differences could be observed between WT,

35S::βI-Gal and the *bgal1/bgal3* double mutant, both in floral stem internodes and in etiolated hypocotyls (Fig S5).

Galactan localization is altered in 35S::βI-Gal and *bgal1/bgal3* plants

β-(1,4)-galactan immunolocalization on cross-sections of WT, 35S::βI-Gal and *bgal1/bgal3* apical internodes with the LM5 antibody revealed an altered distribution of this pectic side chain (Fig. 3a). In transverse sections of 35S::βI-Gal stem a reduction in the detection of the LM5 epitope when compared with WT was apparent in all tissues, particularly in outer epidermal cell walls and pith parenchyma cells. In equivalent transverse sections of *bgal1/bgal3*, there was only a slight increase in LM5 epitope detection in epidermis and cortical parenchyma cell walls when compared with WT.

In WT 4-d-old etiolated hypocotyls LM5 labelling was restricted to the vascular cylinder, as can be seen in sections counterstained with Calcofluor White (Fig. 3b). In *bgal1/bgal3* sections from these organs, a notable galactan increase was detected in epidermis and in parenchyma cells (Fig. 3b). No significant changes could be noticed in 35S::βI-Gal respect to WT.

Amount of KOH-extracted XG varies in relation to galactan levels in 35S::βI-Gal and *bgal1/bgal3* elongating organs

Since our results point to a relation of elongation with β-(1-4)-galactan, one of the main side chain of RGI, and since it was proposed that different cell wall polysaccharides, namely cellulose, xyloglucan and pectins interact with each other, we study the level of different xyloglucan epitopes in plants with altered level of β-(1,4)-galactan, both 35S:: βI-Gal transgenic plants and *bgal1/bgal3* double mutant in relation to WT. Thus, the KOH-extracted fraction was analysed by the EDC method using a set of monoclonal antibodies against different xyloglucan (XG) epitopes in order to establish a possible correlation between specific XG substitutions and their interactions with other cell wall components.

As seen in Fig. 4, XG elutes in the early fractions due to its neutral charge. In apical floral stem internodes (Fig. 4a) 35S::βI-Gal plants showed a decrease in XG detected with LM25 (which recognized XLLG, XXLG and XXXG), CCRC-M1 (XXFG) and CCRC-M58 (XLLG) (Fig. 4a). Others antibodies used, CCRC-M100, which recognizes XG with no substitutions in xylose residues (XXXG)

and CCRC-M101, specific for XG with xylose substitutions, did not indicate any change (Fig. S6). In *bgal1/bgal3* floral stem internodes, only LM25 showed differences when compared with the WT, recognizing an additional XG subpopulation (fractions 26 to 32) that was not detected with other XG antibodies, as can be seen for CCR-M1 or CCRC-M58 (Fig. 4a). Profiles for the rest of CCRC antibodies recognizing XG epitopes are included in Fig. S6.

In-35S::βI-Gal 4-d-old hypocotyls, XG levels do not vary between the transgenic plants an the WT (Fig. 4b and S6) consistently with the absence of changes in galactan levels. Four-d-old hypocotyls displayed differences between *bgal1/bgal3* and WT in KOH-extracted XG (Fig. 4b), as happen in apical internodes. Thus, a XG increase was detected in the double *bgal1/bgal3* mutant hypocotyls, both with LM25 and with CCRC antibodies specific for XG with xylose substitutions (CCRC-M58 and CCRC-M101) (Fig. 4b), while no differences were found in profiles obtained for CCRC-M1 (fucosylated XG) and CCRC-M100 (unsubstituted xylose, XXXG) (Fig. S6).

Changes in KOH-extracted XG in 35S::βI-Gal and *bgal1/bgal3* plants are derived from changes in XG entrapped within cellulose microfibrils

In order to establish whether the changes in KOH-extracted XG could be related to variations in the levels of XG entrapped within cellulose microfibrils, we analysed the cellulosic fraction obtained after the cell wall sequential extraction with H_2O, CDTA and KOH. This cellulosic fraction was treated with a cellulose specific endoglucanase and the polysaccharides released were analysed by ELISA with the XG specific antibodies directed against XG with xylose substitutions and against XG with unsubstituted xylose. Likewise, anti-xylan/arabinoxylan LM11 antibody was also used as comparative epitope, with no differences between mutant/transgenic plants and WT (Fig. 5). No detectable levels of any epitope analyzed were detected in untreated controls. To confirm the total release of XG from the cellulosic fraction, the neutral monosaccharide composition of residue obtained after enzyme treatment was analysed by gas chromatography. No xylose was detected in any of the samples analysed (Fig. S7), thus confirming the absence of XG in the residue obtained after the endoglucanase treatment. The higher content of Man and Ara in the residue of 35S::βI-Gal floral stem internodes when compared to WT or *bgal1/bgal3*, could be pointing to a stronger interaction of

manose and arabinose containing polysaccharides with cellulose induced by the loss of galactan in 35S::βI-Gal internodes.

Analysis of the XG released from the cellulosic fraction with endoglucanase treatment of apical internodes (Fig. 5a), revealed that 35S:: βI-Gal plants showed a slight increase in LM25 and CCRC-M1 epitopes, while CCRC-M58 and CCRC-M100 displayed reduced or similar levels, respectively, to those found in WT. The most noticeable changes were found for CCRC-M101 epitope (XG with xylose substitutions) whose signal was greatly increased (almost two-fold). Contrary *bgal1/bgal3* internodes showed reduced levels of all XG epitopes analysed, except for the CCRC-M100 antibody (specific for XXXG epitope) (Fig. 5a).

Polysaccharides released from the cellulosic fraction of *bgal1/bgal3* hypocotyls (Fig. 5b) showed reduced levels of all XG epitopes analysed. This reduction was especially noticeable for XG with xylose substitutions recognized by CCRC-M1, CCRC-58 and CCRC-101 antibodies, showing a three-fold decrease for fucosylated XXFG motifs (CCRC-M1) and a two-fold decrease for galactosylated XLLG motifs (CCRC-M58). No significant changes could be observed in any of the XG epitopes analysed in etiolated hypocotyls of 35S::βI-Gal plants (Fig. 5b).

Discussion

β-(1,4)-galactan level changes during cell elongation in the Arabidopsis floral stem and etiolated hypocotyl.

β-(1,4)-galactan is a major side chain of RGI. Although the specific function of this polymer has not been completely established, it has been related to different process, such as cell elongation, fiber differentiation or fruit ripening (Willats et al. 2001). To assess the role of this polymer during cell elongation and cell wall organization, Arabidopsis plants with reduced β-(1,4)-galactan side chains (35S::βI-Gal, overproducing chickpea βI-Gal β-galactosidase) or increased β-(1,4)-galactan level (*bgal1/bgal3*, a double mutant for Arabidopsis BGAL1 and BGAL3 β-galactosidases) have been successfully generated (Figs. S2, S3, S4, Fig. 2).

The phenotypic characterization of these plants showed that only the double *bgal1/bgal3* mutant displayed an altered growth phenotype (Fig. 1, Fig. S3), whereas no evident differences between 35S::βI-Gal and WT plants were detected, with no drastic alterations in growth or morphology (Fig. S3). The double *bgal1/bgal3* mutant, where BGAL1 and BGAL3 proteins were absent and a subsequent increase in β-(1,4)-galactan was noted (Fig. 2, 3), present a reduction in the length of the actively growing organs, such as the apical internodes of the floral stem (Fig. 1a) and etiolated hypocotyls (Fig. 1b). Several studies have proposed a relationship between galactan levels and elongation in other systems. Early studies on the role of β-(1,4)-galactan in cell wall dynamics pointed to a direct implication of galactan turnover in elongation of legume epicotyls, stems and roots (Tanimoto 1988; Martín et al. 2013). Similarly, in cell cultures of *Populus alba* β-(1,4)-galactan turnover has been observed during cell elongation (Kakegawa et al. 2000) and metabolism of this neutral side chain seems to be related also to cell elongation in Arabidopsis roots (McCartney et al. 2003).

The lack of phenotypic changes in hypocotyls in 35S::βI-Gal plants could be explained by the very low levels of β-(1,4)-galactan (Fig. 2b) in the cell walls from these organs. Nor is it surprising the absence of a severe growth phenotype in 35S::βI-Gal floral stem, despite the marked reduction in galactan content of elongating apical internodes (Fig. 2a, 3a, Tab.1), since several studies have reported that reducing the galactose content in the cell wall does not produce severe morphological changes (Sorensen et al. 2000; Martín et al. 2005). Only in Arabidopsis plants overexpressing a fungal endo-β-(1,4)-galactanase, with a marked decrease in galactan side chains, a slight delay in the floral stem elongation and a reduction in its diameter were observed (Obro et al. 2009).

Considering our results, it seems that the level of pectic galactan could affect cell elongation in Arabidopsis floral stem and etiolated hypocotyls. Besides, the galactan increase in *bgal1/bgal3* plants detected by EDC (Fig. 2a, b) is localized in the outer parenchyma layers and in epidermal cells (Fig. 3a, b), especially noticeable in 4-d-old hypocotyls. Since the epidermis is a key tissue in the control of elongation (Bret-Harte and Talbott 1993), the changes caused by the double mutation *bgal1/bgal3* mutant in the galactan level (Fig. 3b), could explain the lower length of hypocotyls and internodes and reinforces the fact that cell wall galactan levels affect cell elongation. Furthermore, these results point to an specific action of these two arabidopsis β-galactosidases (BGAL1 and BGAL3) in the cell wall galactan turnover in epidermal cells. Any action of these β-galactosidases in other containing

galactose cell wall polymer, such as the beta-linked galactose in xyloglucan has been ruled out, since BGAL10 was identified as the only Arabidopsis β-galactosidases active against XG (Sampedro et al. 2012). Also the specificity of chickpea βI-Gal and its lack of activity against have been determined (Hernández-Nistal, personal communication).

It is noteworthy that in the case of the apical internodes the galactan increase in *bgal1/bgal3* mutant is only detected in the more acidic population of the CDTA fraction (Fig. 2a), previously identified as the one co-eluting with the pectic macromolecule including unesterified homogalacturonan domains (Cornuault et al. 2014), which could be reflecting a specific action of BGAL1 and BGAL3 proteins in certain pectic domains within the cell wall to carry out their function during elongation of this organ. Our results also indicate that Arabidopsis BGAL1 and BGAL3 β-galactosidases act cooperatively to reduce β-(1,4)-galactan levels during cell elongation in etiolated hypocotyls and elongating internodes, since single *bgal1* and *bgal3* mutants did not show any growth phenotype or detectable alterations in their galactan levels (Moneo-Sánchez et al. 2018).

XG structure is influenced by under- or over-expression of pectic β-(1,4)-galactosidases

The role of pectins in cell wall organization and remodelling during cell elongation has been extensively discussed in the different cell wall models proposed through the years (Talbott and Ray 1992; Carpita and Gibeaut 1993; Vincken et al. 2003). Recent studies have reported evidence for pectin/XG and pectin/cellulose interactions through RGI neutral side chains (Popper and Fry 2008; Lin et al. 2015). Indeed, based on *in vitro* systems, a direct competition between pectins and XG to bind cellulose has been proposed, so that when pectin/XG ratio is high, pectic polysaccharides bind to cellulose preferentially (Zykwinska et al. 2008) and may limit the access of XG to cellulose microfibrils (White et al. 2014). All these interactions must be considered to understand cell wall architecture and the different polysaccharide networks controlling cell wall turnover during development.

In the two experimental systems developed in this work, in which we have modified RGI galactan side chains: reducing them in the case of 35S::βI-Gal plants and increasing them in the case of *bgal1/bgal3* (Fig. 2), we found a direct correlation between the galactan levels and the level of KOH-extracted XG (Fig. 4), both decreased in plants producing βI-Gal and enhanced in the double mutant

(in both cases XG with xylose bound substitutions), thus reflecting the importance of RGI side chains in the XG extractability, probably modifying the cellulose/XG interactions.

We have to take into account that, although KOH extracts the XG fraction interacting with the surface of the cellulose microfibrils, part of the XG, trapped between cellulose microfibrils, possibly during microfibril synthesis, can not be extracted until cellulose is degraded (Pauly et al. 1999; Park and Cosgrove 2015). The analysis of the XG released after cell wall hydrolysis with a cellulose-specific endoglucanase (Fig. 4, 5) indicated that when XG levels increase in the KOH fraction, (accompanied by an increase in β-(1-4)-galactan in *bgal1/bgal3* plants), they decrease in the cellulosic fraction and *vice versa* in 35S::βI-Gal plants, supporting the hypothesis that could be a direct competition between the neutral side chains of the pectins and the XG for binding to cellulose, which determines the proportion of the XG binding to the surfaces of the microfibrils and the amount of XG trapped between them.

Moreover, our results suggest that the cellulose/XG interactions may be occurring preferentially through the substitutions attached to xylose residues of the XG molecule, as all changes in XG extractability (both in KOH and cellulosic fractions), are detected with antibodies directed against these XG motifs, as CCRC-M1, CCRC-M58, and CCRC-M101 (Fig. 5a, b), an minor or no variations are found with CCRC-M100, specific for XXXG. In the case of 35S::βI-Gal internodes, CCRC-M101 epitope shows the highest variation in the cellulosic fraction, although no variations in this epitope are observed in the KOH extracts. This may be suggesting a differential pattern of xylose substitutions implied in cellulose-XG interactions in both fractions that in turn results in a differential XG extractability. However, taking bgal1/bgal3 results into account, we cannot confirm that these bounds are exclusively through fucose substitutions, as proposed by some authors based on *in vitro* studies (Levy et al. 1997; Lima et al. 2004). This could be due to the plant material used in our study (young, actively elongating organs), since the cellulose binding capacity of the fucosylated or non-fucosylated XG depend on the degree of crystallinity of the cellulose (Chambat et al. 2005), being both forms of XG able to bind to cellulose from primary cell walls, present in elongating organs. We can not exclude the possibility that general galactose metabolism could be altered due to greater or lesser amounts of galactose being re-incorporated into the cell as a result of higher or lower galactosidase activity. However, although it can be consider that the repression or increase of galactan degradation may

alter the galactose available for synthesis of XG side chains, it is clear that the observed galactan changes mediated by the studied β-galactosidases influence XG structure in muro.

In conclusion, this work points to a role of β-(1,4)-galactan in cell growth at least in Arabidopsis etiolated hypocotyls and floral stems, and allows us to propose that BGAL1 and BGAL3 β-galactosidases act in a coordinate way during this process. Our results also indicate that XG structure is influenced by under- or over-expression of pectic β-(1,4)-galactosidases and that the level of β-(1,4)-galactan may affect the degree of interaction between cellulose and XG, a factor that is likely to play a crucial role in cell wall architecture.

Author contribution statement

IM, BD and EL conceived and designed research. MM-S and AA-C conducted experiments. IM wrote the manuscript. JPK help with the EDC analysis and with the discussion of the results. All authors read and approved the manuscript.

References

Ahn YO, Zheng M, Bevan DR, Esen A, Shiu SH, Benson J, Peng HP, Miller JT, Cheng CL, Poulton JE, Shih MC (2007) Functional genomic analysis of *Arabidopsis thaliana* glycoside hydrolase family 35. Phytochem 68:1510-1520

Albersheim P, Nevins DJ, English PD (1967) A method for the analysis of sugars in plant cell wall polysaccharides by gas liquid chromatography. Carbohydr Res 5:340-345

Albornos L, Martín I, Pérez P, Marcos R, Dopico B, Labrador E (2012) Promoter activities of genes encoding β-galactosidases from Arabidopsis a1 subfamily. Plant Physiol 60:223-232

Alonso JM, Stepanova AN, Leisse TJ, Kim CJ, Chen H, Shinn P et al. (2003) Genome-wide insertional mutagenesis of *Arabidopsis thaliana*. Sci 301:653-657

Bret-Harte MS, Talbott LD (1993) Changes in composition of the outer epidermal cell wall of pea stems during auxin-induced growth. Planta 190:369-378

Carpita NC, Gibeaut DM (1993) Structural models of primary cell walls in flowering plants: consistency of molecular structure with the physical properties of the walls during growth. Plant J 3:1-

Chambat G, Karmous M, Costes M, Picard M, Joseleau JP (2005) Variation of xyloglucan substitution pattern affects the sorption on celluloses with different degrees of crystallinity. Cellulose 12:117-125

Clough SJ, Bent AF (1998) Floral dip: a simplified method for *Agrobacterium*-mediated transformation of *Arabidopsis thaliana*. Plant J 16:735-743

Cornuault V, Manfield IW, Ralet M-C, Knox JP (2014) Epitope detection chromatography: a method to dissect the structural heterogeneity and inter-connections of plant cell-wall matrix glycans. Plant J 78:715-722

Cosgrove DJ (2016) Plant cell wall extensibility: connecting plant cell growth with cell wall structure, mechanics, and the action of wall modifying enzymes. J Exp Bot 67:463-476

Dick-Pérez M, Zhang Y, Hayes J, Salazar A, Zabotina OA, Hong M (2011) Structure and interactions of plant cell-wall polysaccharides by two-and three-dimensional magic-angle-spinning solidstate NMR. Biochem 50:989-1000

Esteban R, Labrador E, Dopico B. (2005) A family of β-galactosidase cDNAs related to development of vegetative tissue in *Cicer arietinum*. Plant Sci 168:457-466

Hayashi T (1989) Xyloglucans in the primary cell wall. Annu Rev Plant Physiol 40:139-168

Kakegawa K, Edashige Y, Ishii T (2000) Metabolism of cell wall polysaccharides in cell suspension cultures of *Populus alba* in relation to cell growth. Physiol Plant 105:420-425

Karimi M, Depicker A, Hilson P (2007) Recombinational cloning with plant gateway vectors. Plant Physiol 145:1144-1154

Levy S, Maclachlan G, Staehelin LA (1997) Xyloglucan sidechains modulate binding to cellulose during *in vitro* binding assays as predicted by conformational dynamics simulations. Plant J 11:373-386

Lima DU, Loh W, Buckeridge MS (2004) Xyloglucan-cellulose interaction depends on the sidechains and molecular weight of xyloglucan. Plant Physiol Biochem 42:389-394

Lin D, Lopez-Sanchez P, Gidley MJ (2015) Binding of arabinan or galactan during cellulose

synthesis is extensive and reversible. Carbohydr Polym 126:108-121

Martín I, Dopico B, Muñoz FJ, Esteban R, Oomen RJFJ, Driouich A, Vincken JP, Visser R, Labrador E (2005) *In vivo* expression of a *Cicer arietinum* β-galactosidase in potato tubers leads to a reduction of the galactan side-chains in cell wall pectin. Plant Cell Physiol 46:1613-1622

Martín I, Hernández-Nistal J, Albornos L, Labrador E, Dopico B (2013) βIII-Gal is involved in galactan reduction during phloem element differentiation in chickpea stems. Plant Cell Physiol 54:960-970

Martín I, Jiménez T, Esteban R, Dopico B, Labrador E (2008) Immunolocalization of a cell wall β-galactosidase reveals its developmentally regulated expression in *Cicer arietinum* and its relationship to vascular tissue. J Plant Growth Regul 27:181-191

Martín I, Jiménez T, Hernández-Nistal J, Dopico B, Labrador E (2011) The βI-galactosidase of *Cicer arietinum* is located in thickened cell walls such as those of collenchyma, sclerenchyma and vascular tissue. Plant Biol 13:777-783

Martín I, Jiménez T, Hernández-Nistal J, Labrador E, Dopico B (2009) The location of the chickpea cell wall βV-galactosidase suggests involvement in the transition between cell proliferation and cell elongation. J Plant Growth Regul 28:1-11

McCann MC, Roberts K (1991) Architecture of the primary cell wall. In: Lloyd CW (ed) The cytoskeletal basis of plant growth and form. Academic Press, London, pp 109-129

McCartney L, Steele-King CG, Jordan E, Knox JP (2003) Cell wall pectic (1-4)-β-D-galactan marks the acceleration of cell elongation in the Arabidopsis seedling root meristem. Plant J 33:447-454

Miedes E, Zarra I, Hoson T, Herbers K, Sonnewald U, Lorences EP (2011) Xyloglucan endotransglucosylase and cell wall extensibility. J Plant Physiol 168:196-203

Moneo-Sánchez M, Izquierdo L, Martín I, Hernández-Nistal J, Albornos L, Dopico B, Labrador E (2018) Knockout mutants of *Arabidopsis thaliana* β-galactosidase. Modifications in the cell wall saccharides and enzymatic activities. Biol Plant 62:80-88

Moneo-Sánchez M, Izquierdo L, Martín I, Labrador E, Dopico B (2016) Subcellular location of *Arabidopsis thaliana* subfamily a1 β-galactosidases and developmental regulation of transcript levels of their coding genes. Plant Physiol Biochem 109:137-145

Murashige T, Skoog F (1962) A revised medium for rapid growth and bioassays with tobacco tissue cultures. Physiol Plant 15:473-497

Obro J, Borkhardt B, Harholt J, Skjøt M, Willats WG, Ulvskov P (2009) Simultaneous *in vivo* truncation of pectic side chains. Transgenic Res 18:961-969

O'Neill MA, York WS (2003) The composition and structure of plant primary cell walls. In: Rose JKC (ed) The plant cell wall. Blackwell Scientific Publications, Oxford, pp. 1-54

Park YB, Cosgrove DJ (2015) Xyloglucan and its interactions with other components of the growing cell wall. Plant Cell Physiol 56:180-94

Pauly M, Albersheim P, Darvill A, York WS (1999) Molecular domains of the cellulose/xyloglucan network in the cell walls of higher plants. Plant J 20:629-639

Pauly M, Qin Q, Greene H, Albersheim P, Darvill A, York WS (2001) Changes in the structure of xyloglucan during cell elongation. Planta 212:842-850

Peaucelle A, Braybrook S, Höfte H (2012) Cell wall mechanics and growth control in plants: the role of pectins revisited. Front Plant Sci 3:121

Popper ZA, Fry SC (2008) Xyloglucan-pectin linkages are formed intra-protoplasmically, contribute towall assembly, and remain stable in the cell wall. Planta 227:781–794

Sampedro J, Gianzo C, Iglesias N, Guitián E, Revilla G, Zarra I (2012) AtBGAL10 is the main xyloglucan β-galactosidase in arabidopsis, and its absence resuls in unusual xyloglucan subunits and growth defects. Plant Physiol 158: 1146-1157

Sorensen SO, Pauly M, Bush M, Skjot M, McCann MC, Borkhardt B, Ulvskov P (2000) Pectin engineering: modification of potato pectin by *in vivo* expression of an endo-1,4-β-D-galactanase. Proc Natl Acad Sci USA 97:7639-7644

Talbott LD, Ray PM (1992) Changes in molecular size of previously deposited and newly synthesized pea cell wall matrix polysaccharides. Plant Physiol 98:369-379

Tanimoto E (1988) Gibberellin regulation of root growth with change in galactose content of cell walls in *Pisum sativum*. Plant Cell Physiol 29:269-280

Trainotti L, Spinello R, Piovan A, Spolaore S, Casadoro G (2001) β-Galactosidases with a lectin-like domain are expressed in strawberry. J Exp Bot 52:1635-1645

Vincken JP, Schols HA, Oomen RJFJ, McCann MC, Ulvskov P, Voragen AGJ, Visser RGF (2003) If homogalacturonan were a side chain of rhamnogalacturonan I. Implications for cell wall architecture. Plant Physiol 132:1781-1789

Wang T, Park YB, Caporini MA, Rosay M, Zhong L, Cosgrove DJ, Hong M (2013) Sensitivity-enhanced solid-state NMR detection of expansin's target in plant cell walls. Proc Natl Acad Sci USA 110:16444-16449

Wang T, Park YB, Cosgrove DJ, Hong M (2015) Cellulose-pectin spatial contacts are inherent to never-dried *Arabidopsis thaliana* primary cell walls: evidence from Solid-State NMR. Plant Physiol 168:871-884

White PB, Wang T, Park YB, Cosgrove DJ, Hong M (2014) Water-polysaccharide interactions in the primary cell wall of *Arabidopsis thaliana* from Polarization Transfer Solid-State NMR. J Am Chem Soc 136:10399-10409

Willats WGT, McCartney L, Mackie W, Knox JP (2001) Pectin: cell biology and prospects for functional analysis. Plant Mol Biol 47:9-27

Wolf S, Greiner S (2012) Growth control by cell wall pectins. Protoplasma 249:169-175

Zykwinska A, Thibault JF, Ralet MC (2007) Organization of pectic arabinan and galactan side chains in association with cellulose microfibrils in primary cell walls and related models envisaged. J Exp Bot 58:1795-1802

Zykwinska A, Thibault J-F, Ralet M-C (2008) Competitive binding of pectin and xyloglucan with primary cell wall cellulose. Carbohydr Polym 74:957-961

Figure Legends

Fig. 1 Phenotypic characterization of *bgal1/bgal3* plants. (**a**) Length of the different internodes (numbered 1st to 4th from base to apex) and the whole floral stem (Final length) of 38-d-old WT and *bgal1/bgal3* plants. (**b**) Final hypocotyl length of 2- 4- and 7-d-old etiolated WT and *bgal1/bgal3* seedlings. Values are means ± SEM of three biological replicates. The star indicates the levels of significance (Student's t test): *p < 0.05; **p < 0.01.

Fig. 2 EDC profiles for anti-β-(1,4)-galactan LM5 antibodies. (**a**) Profiles for CDTA extracts from cell walls of WT, 35S::βI-Gal and *bgal1/bgal3* apical floral stem internodes. (**b**) Profiles for CDTA extracts from cell walls of WT, 35S::βI-Gal and *bgal1/bgal3* 4-d-old etiolated hypocotyls. Values are means of three biological replicates ± SD.

Fig. 3 β-(1,4)-galactan immunolocalization in 35S::βI-Gal and *bgal1/bgal3* plants with LM5 antibody. (**a**) Cross sections from apical floral stem internodes of WT, 35S::βI-Gal and *bgal1/bgal3* plants. (**b**) Cross sections from 4-d-old etiolated hypocotyls from WT (with LM5 antibodies and counterstained with calcofluor white) and *bgal1/bgal3* seedlings. co: cortex; ep: epidermis; pi: pith parenchyma; vt: vascular tissue.

Fig. 4 EDC profiles for anti-XG antibodies. (**a**) Profiles for LM25 (which recognized XLLG, XXLG and XXXG), CCRC-M1 (XXFG) and CCRC-M58 (XLLG) in KOH extracts from cell walls of WT, 35S::βI-Gal and *bgal1/bgal3* apical floral stem internodes. (**b**) Profiles for LM25, CCRC-M58 and CCRC-M101 (XG with xylose substitutions) in KOH extracts from cell walls of WT, 35S::βI-Gal and *bgal1/bgal3* 4-d-old etiolated hypocotyls. Values are means of three biological replicates ± SD.

Fig. 5 ELISA analysis of polysaccharides released after treatment of the cellulosic fraction from WT, 35S::βI-Gal and *bgal1/bgal3* plants with a cellulose specific endoglucanase. Results are shown for antibodies against XG with xylose substitutions [LM25 (which recognized XLLG, XXLG and XXXG), CCRC-M1 (XXFG), CCRC-M58 (XLLG) and CCRC-M101], XG with no xylose substitutions [CCRC-M100 (XXXG)] and xylan/arabinoxylan [LM11]. (**a**) ELISA signal from cell walls of WT, 35S::βI-Gal and *bgal1/bgal3* apical floral stem internodes. (**b**) ELISA signal from cell walls of WT, 35S::βI-Gal and *bgal1/bgal3* 4-d-old etiolated hypocotyls. Values are means ± SD of three biological replicates. The star indicates the levels of significance (Student's t test): *p < 0.05; **p < 0.01.

Figure 1

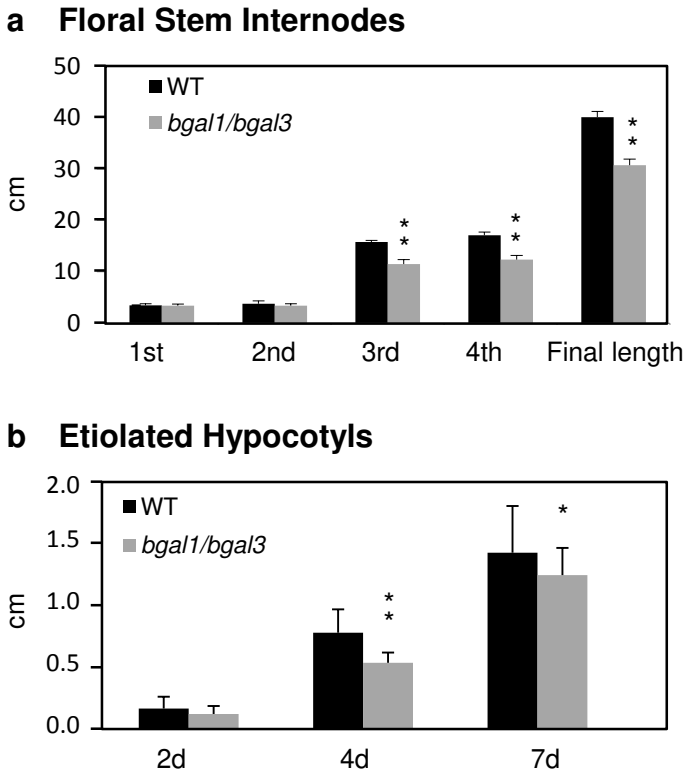

Fig. 1

a **Floral Stem Internodes**

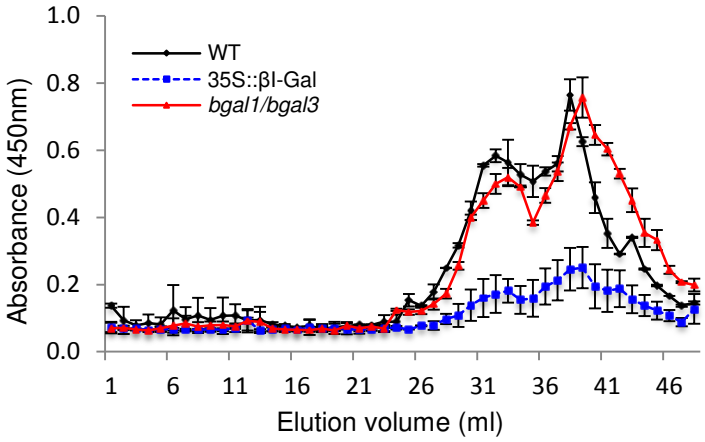

b **Etiolated Hypocotyls**

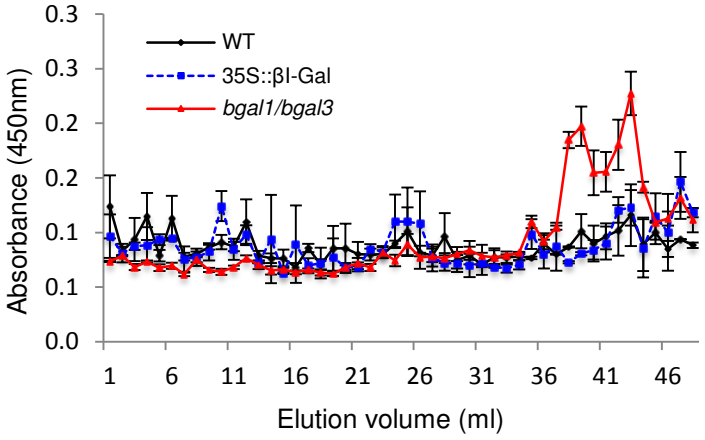

Fig. 2

Figure 3

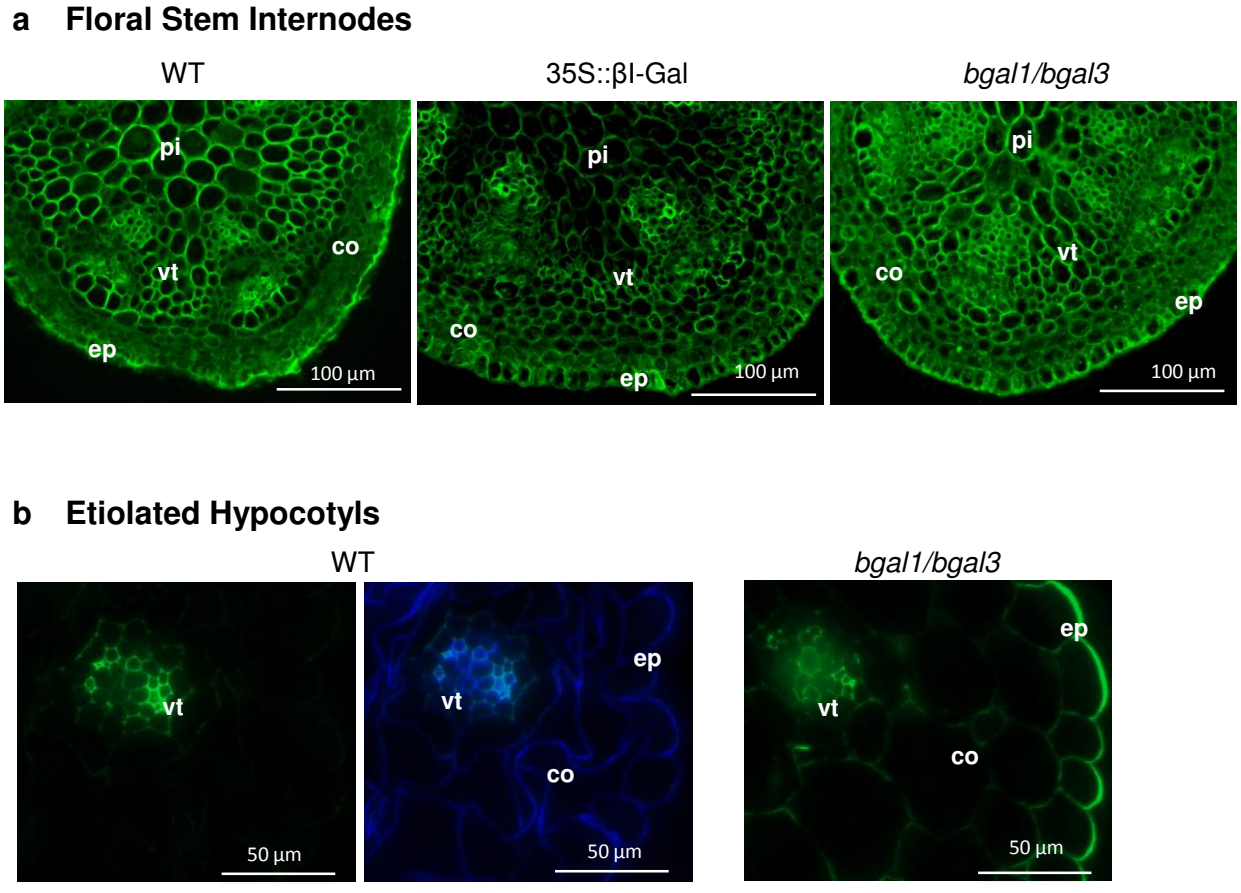

Fig. 3

Figure 4

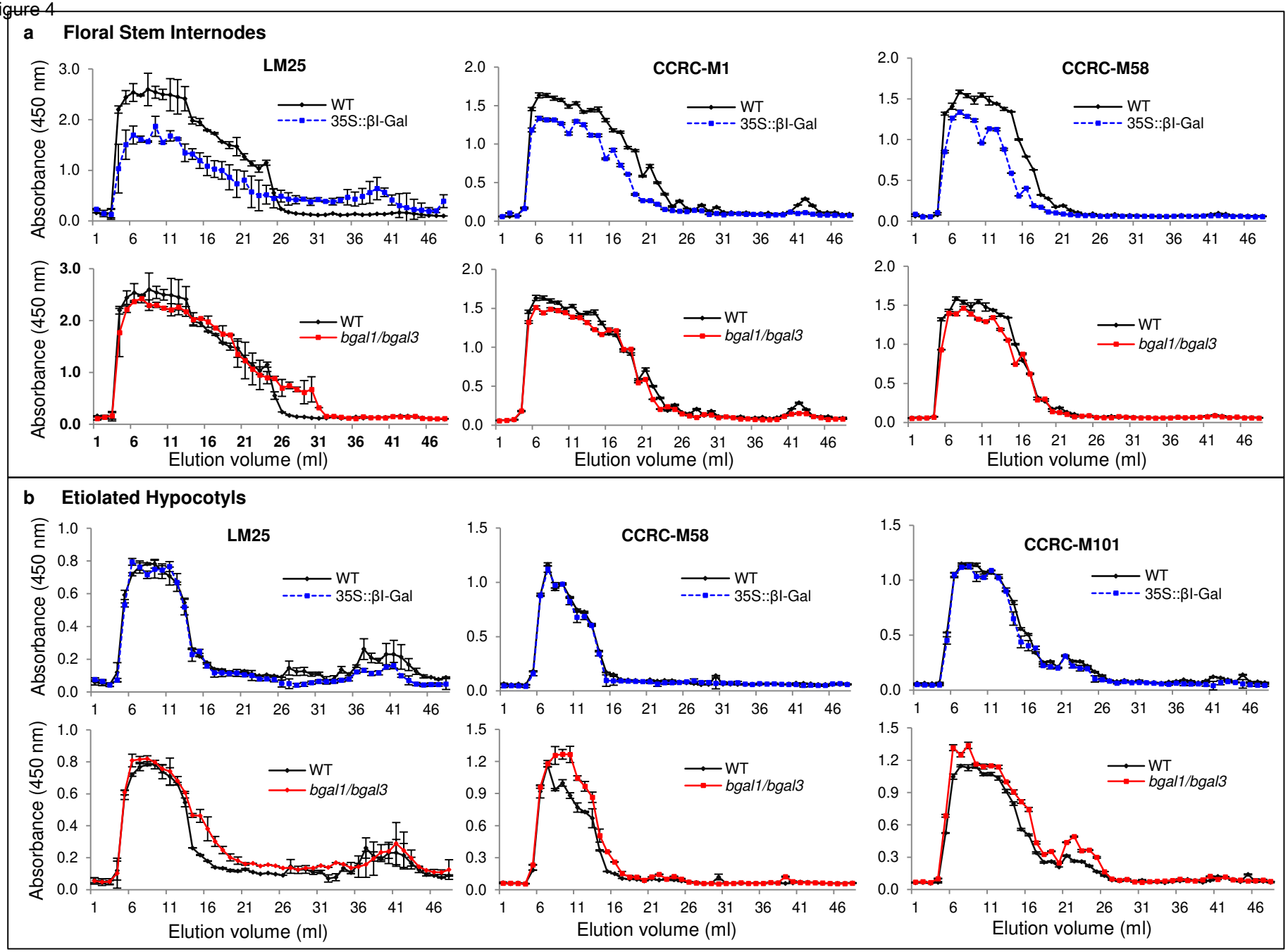

Fig. 4

Figure 5

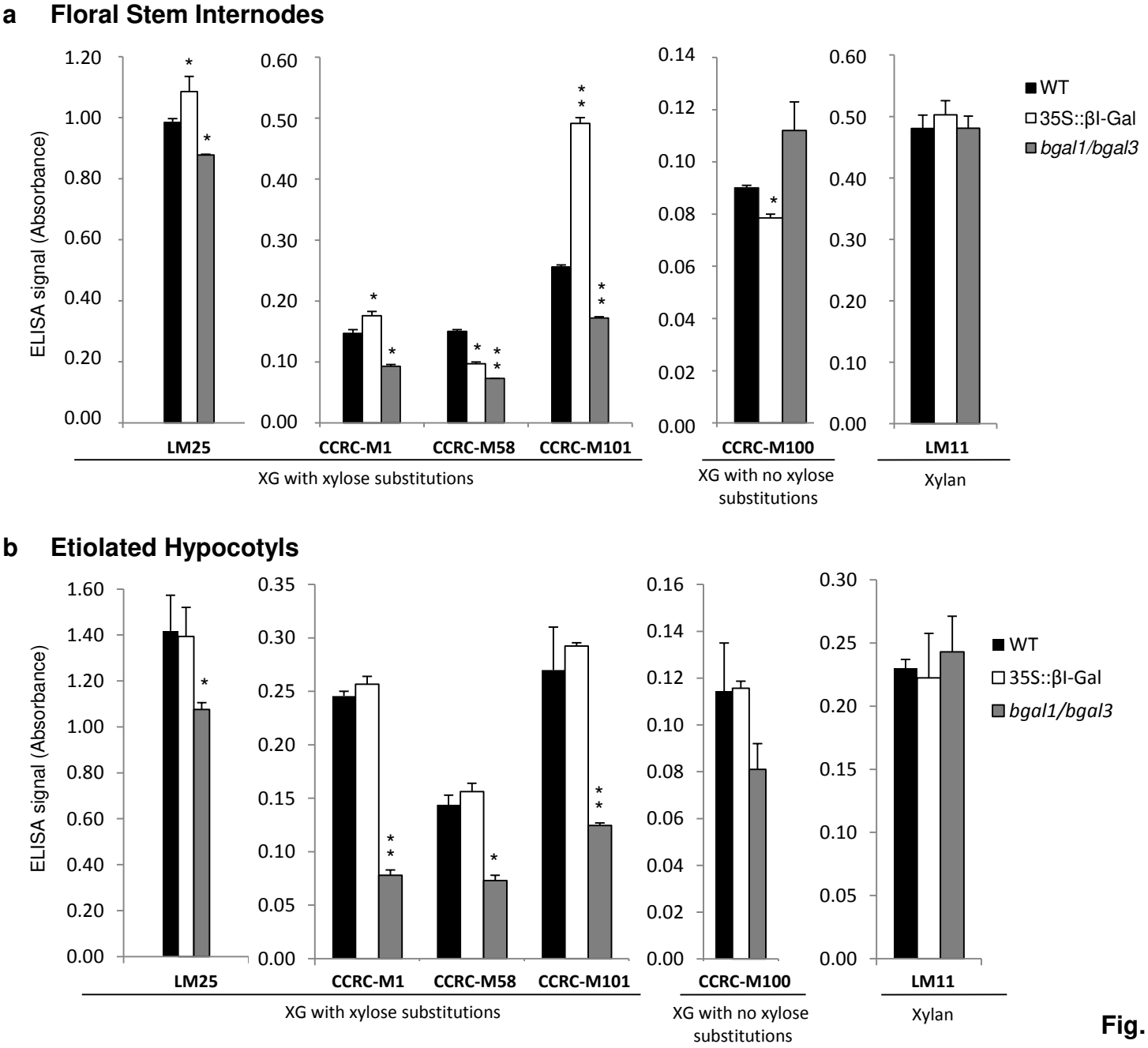

Fig. 5

Table 1

Table 1. Galactose content (expressed as %) in cell walls from WT, 35S::βI-Gal and *bgal1/bgal3* Floral Stem Internodes and 4-d-old Etiolated Hypocotyls.Values are means ± SEM of three biological replicates. The stars indicates the levels of significance (Student's t test): *$p < 0.05$; **$p < 0.01$.

	Galactose (%)		
	WT	**35S::βI-Gal**	***bgal1/bgal3***
Floral Stem Internodes	17.79±0.22	10.79±2.74*	31.44±0.21**
Etiolated Hypocotyls	30.46±3.14	32.51±0.92	39.79±3.75*